Journal of Dental Sciences 18 (2023) 237–247

Available online at www.sciencedirect.com

ScienceDirect

journal homepage: www.e-jds.com

Original Article

Circ_0004491 stimulates guanine nucleotide-binding protein alpha subunit to inhibit the malignant progression of oral squamous cell carcinoma by sponging miR-2278

Tao Cheng [a*,1], Feifei Huang [b,1], Yin Zhang [a], Zhen Zhou [a]

[a] *Department of Stomatology, Hanyang Hospital Affiliated to Medical College of Wuhan University of Science and Technology, Wuhan, China*
[b] *Department of Respiratory Medicine, Dongxihu District People's Hospital of Wuhan City in Hubei Province, Wuhan, China*

Received 15 April 2022; Final revision received 24 May 2022
Available online 15 June 2022

KEYWORDS
circ_0004491;
GNAS;
miR-2278;
Oral squamous cell carcinoma

Abstract *Background/purpose:* Circular RNA origin recognition complex subunit 4 (circORC4; ID: hsa_circ_0004491) have been confirmed to be a novel potential biomarker of oral squamous cell carcinoma (OSCC). This study aimed to explore the molecular mechanism of circ_0004491 in OSCC progression.
Materials and methods: Levels of circ_0004491, microRNA (miR)-2278, guanine nucleotide-binding protein alpha subunit (GNAS), Bax, Bcl-2, E-cadherin and ki-67 were detected by quantitative real-time PCR, western blotting and immunohistochemistry. The proliferation of OSCC cells was measured using colony formation assay and EdU staining. Cell apoptosis and motility were detected by flow cytometry and transwell assays respectively. Interaction between miR-2278 and circ_0004491 or GNAS was predicted by bioinformatics analysis and confirmed via luciferase reporter assay and RNA immunoprecipitation assay. Xenograft tumor model was used to analyze the role of circ_0004491 in tumor growth *in vivo*.
Results: Circ_0004491 was downregulated in OSCC tissues and cell lines. Circ_0004491 overexpression suppressed the proliferation, migration and invasion whereas facilitated the apoptosis of OSCC cells. Circ_0004491 acted as a molecular sponge for miR-2278, and circ_0004491 overexpression-mediated effect was partly reversed by miR-2278 mimic in OSCC cells. MiR-2278 interacted with the 3'UTR of GNAS. Circ_0004491 contributed to GNAS level by sponging

* Corresponding author. Department of StomatologyHanyang Hospital Affiliated to Medical College of Wuhan University of Science and Technology, No. 53, Ink Lake Road, Hanyang District, Wuhan, 430050, China.
E-mail address: chengtao202108@126.com (T. Cheng).
[1] These two authors contributed equally to this work.

https://doi.org/10.1016/j.jds.2022.05.018

miR-2278 in OSCC cells. GNAS knockdown restored miR-2278 inhibitor-mediated effect in OSCC cells. Circ_0004491 overexpression repressed xenograft tumor growth *in vivo*.
Conclusion: Circ_0004491 can repress OSCC progression by regulation of miR-2278/GNAS axis, providing a possible circRNA-targeted therapy for OSCC.

Introduction

Oral squamous cell carcinoma (OSCC) is an increasingly fatal malignant tumor, which originated from the lesions of oral mucosal epithelial tissue.[1,2] The main characteristics of OSCC are lymphatic metastasis and distant metastasis, which seriously affect the patient's quality of life.[3] The current treatment strategy for OSCC is surgery combined with radiotherapy and chemotherapy.[1,4] The current treatment strategy is only effective for early stage patients. For advanced patients, the cure rate was significantly decreased and the risk of recurrence was increased.[5,6] Therefore, there is an urgent need to explore the pathogenesis of OSCC in depth, and provide a new basis for finding effective biomarkers and therapeutic targets for diagnosis and treatment.

Circular RNA (circRNA) is a conserved endogenous noncoding RNA that is widely expressed in multiple species.[7] The ring structure formed by covalent sealing makes it resistant to RNase-induced degradation and have stronger stability than linear RNA.[7,8] In addition, high-throughput sequencing results showed that circRNA has a different expression pattern in cancer tissues and cells comparing to the controls.[9] Mechanism studies have proved that circRNA contains conserved miRNA target binding sites and was considered as an effective miRNA sponge.[7] For example, hsa_circRNA_100290 contributed to glucose transporter-1 (GLUT1) expression and repressed OSCC cell growth and glycolysis via targeting miR-378a.[10] Therefore, based on the characteristics such as sequence conservation, structural stability and expression difference, circRNA was often used as a biomarker for cancer diagnosis or targeted therapy.[11,12]

Circ_0004491, has been shown to be evidently down-regulated in OSCC tumor tissues and cells in previous studies, and knockdown or overexpression of circ_0004491 could obviously promote or inhibit the motility of OSCC cells.[13] However, the specific molecular mechanism of circ_0004491 involved in the progression of OSCC was still unclear. MiR-2278 was the only potential target miRNA of circ_0004491 retrieved from the starBase online website. In addition, studies have confirmed that miR-2278 was remarkably up-regulated in ovarian cancer[14] and prostate cancer,[15] and played a tumor-promoting effect. Guanine nucleotide-binding protein alpha subunit (GNAS) was predicted to be a candidate target of miR-2278 by the starBase online website. GNAS, one of the G Protein activation subunits, could regulate cellular signaling pathways by encoding Gα.[16] Additionally, Zhu et al. confirmed that GNAS expression in OSCC was evidently lower than that of the control, and it was regulated by circRNA_100533 via absorbing miR-933.[17] However, it was still unclear whether there was a circ_0004491/miR-2278/GNAS axis in the process of OSCC.

Therefore, this study first investigated the role of circ_0004491 in OSCC, and then further verified the involvement of miR-2278/GNAS axis in the regulating effect of circ_0004491 in OSCC progression.

Materials and methods

Clinical tissues and cell lines

59 pairs of OSCC tumor and adjacent normal tissues specimens from Hanyang Hospital Affiliated to Medical College of Wuhan University of Science and Technology were enrolled in this study. All patients had not received chemotherapy or radiation therapy and signed the written informed consent. After operation, all tissue specimens were immediately frozen at −-80 °C. This study was approved by the approval from Hanyang Hospital Affiliated to Medical College of Wuhan University of Science and Technology.

Human oral keratinocyte cell line (HOK) and OSCC cell lines (CAL-27 and HSC-6) were brought from Tongpai Biotechnology (Shanghai, China). SCC-9 and OECM1 cells were purchased from Crisprbio (Beijing, China). CAL-27, SCC-9, HSC-6 and HOK cells were cultured in DMEM (Gibco, Rockville, MD, USA), and OECM-1 cells were incubated in RPMI-1640 (Gibco) at 37 °C with 5% CO_2. 10% fetal bovine serum (FBS; Gibco) and 1% penicillin/streptomycin (Gibco) were added in mediums.

Quantitative real-time PCR (qRT-PCR)

TRIzol Reagent (Invitrogen, Carlsbad, CA, USA) was used to extract total RNA. Then, NanoDrop One/OneC (Thermo Scientific, Shanghai, China) and High Capacity cDNA Reverse Transcription Kit (Invitrogen) were separately used to examine RNA concentration and obtain cDNA. Finally, the cDNA was mixed with specific primers and SYBR Green (Solarbio, Beijing, China) to conduct qRT-PCR. Relative expression was normalized by U6 small nuclear 1 (RNU6) or glyceraldehyde-phosphate dehydrogenase (GAPDH) and calculated by $2^{-\Delta\Delta CT}$ method. Primer sequences were shown in Table 1.

Table 1 Primers sequences used for PCR.

Name		Primers for PCR (5'–3')
circ_0004491	Forward	AGTGAGCTGCTGAAAAGAACTG
	Reverse	GCTCCAGGCTTCCATAGTTT
ORC4	Forward	CAGCAAAAACCTGCGGTCAT
	Reverse	TGCTACACAGTTGGCTTGCT
miR-2278	Forward	GTATGAGGAGAGCAGTGTGTGTT
	Reverse	CTCAACTGGTGTCGTGGAG
GNAS	Forward	GCAGAAGGACAAGCAGGTCT
	Reverse	TTCTCACCATCGCTGTTGCT
GAPDH	Forward	GACAGTCAGCCGCATCTTCT
	Reverse	GCGCCCAATACGACCAAATC
U6	Forward	CTCGCTTCGGCAGCACA
	Reverse	AACGCTTCACGAATTTGCGT

ORC4: origin recognition complex subunit 4; miR: microRNA; GNAS: guanine nucleotide-binding protein alpha subunit; GAPDH: glyceraldehyde-phosphate dehydrogenase.

Identification of circRNA

In RNase R assay, the RNA extracted from CAL-27 and SCC-9 cells was co-incubated with 3 U/μg RNase R (Geneseed, Guangzhou, China) or equal volume of the 1 × ×Reaction Buffer (Geneseed) for 30 min at 37 °C. Then circ_0004491 expression and linear ORC4 mRNA expression were measured by qRT-PCR. In Actinomycin D (ActD) assay, CAL-27 and SCC-9 cells were co-incubated with ActD solution (Seebio, Shanghai, China) for 0, 4, 8, 12 and 24 h. Then, the RNA was isolated, and qRT-PCR was used to determine circ_0004491 expression and linear ORC4 mRNA expression.

Cell transfection

Circ_0004491 overexpression plasmid (circ_0004491), miR-2278 mimic (miR-2278), miR-2278 inhibitor (in-miR-2278), GNAS shRNA (sh-GNAS) and related controls (vector, miR-NC, in-miR-NC and sh-NC) were designed and synthesized by Ribobio (Guangzhou, China). Lipofectamine 3000 (Invitrogen) was used to perform transfection.

Colony formation assay

Transfected OSCC cells were cultured at 37 °C for 14 days. After removed the cell medium, the colonies were fixed by 4% paraformaldehyde (Phygene, Fuzhou, China) and stained by crystal violet (Phygene), respectively. Then, the number of colonies containing more than 50 cells were counted using an inverted microscope.

EdU staining

EdU staining was conducted to measure OSCC cells growth using BeyoClick™ EdU Cell Proliferation Kit with Alexa Fluor 488 (Beyotime, Shanghai, China). Briefly, CAL-27 and SCC-9 cells were incubated with click reaction buffer, CuSO4, Azide 488, click additive solution and Hoechst 33342 solution. EdU positive cell rate was reflected by the percentage of green signal (EdU positive cells) to blue signal (Hoechst positive cells).

Flow cytometry

Transfected OSCC cells were harvested after culturing for 24 h for the processes recommended by the instructions of the Annexin V-FITC/PI apoptosis detection kit (Roche, Basel, Switzerland). Then, cells were suspended with Binding buffer, and cell suspensions were incubated with 10 μL of Annexin V-FITC and 10 μL of PI for 15 min in the dark. Under a flow cytometer, cell apoptotic rate was assessed.

Transwell assay

To measure the migration and invasion abilities of OSCC cells, transfected cells (5×10^4 cells/well) suspended with serum-free medium were pipetted over the upper of Transwell chambers (Corning, Madison, NY, USA), and culture medium containing 10% FBS was pipetted into the bottom chambers. For invasion assay, cells needed to invade the polycarbonate transwell filter coated with Matrigel (Corning). 24 h later, migrated or invaded cells were fixed with paraformaldehyde (Phygene) and stained with 0.1% crystal violet (Phygene). Migrated and invaded cells were counted under a microscope (100 ×).

Western blotting

RIPA buffer (Beyotime) was used to obtain total protein of OSCC tissues and cells. Then, the protein was separated by SDS-PAGE gel and transferred to PVDF membranes (Bio-Rad, Hercules, CA, USA). After being blocked with 5% defatted milk for 1 h, the protein signals of the membranes were visualized by BeyoECL Plus kit (Beyotime) after co-incubated with primary and secondary antibodies presented in Table 2 at 4 °C overnight. Image Lab software was used to analyze the gray value of proteins. The antibodies were originally provided by Abcam (Cambridge, UK) and Proteintech (Wuhan, China).

Bioinformatics analysis and dual-luciferase reporter system

The online software starBase (http://starbase.sysu.edu.cn/) were used to retrieve the miRNA binding sites in circ_0004491 and GNAS. Fragments of wild or mutant type

Table 2 The antibodies in Western blotting and IHC.

Antibody	Cat.	Dilution ratio	Source
Bax	ab32503	1:10000	Abcam
Bcl-2	ab32124	1:1000	Abcam
E-cadherin	20874-1-AP	1:10000	Proteintech
GNAS	ab283266	1:1000	Abcam
GAPDH	10494-1-AP	1:50000	Proteintech
ki-67	ab15580	1:200	Abcam
Goat Anti-Rabbit IgG H&L (HRP)	ab6721	1:20000	Abcam

Bax: Bcl-2-like protein 4; Bcl-2: B-cell lymphoma 2; GNAS: guanine nucleotide-binding protein alpha subunit; GAPDH: glyceraldehyde-phosphate dehydrogenase.

circ_0004491 and wild or mutant type 3'UTR of GNAS mRNA were cloned into the upstream of pmirGLO luciferase reporter to manufacture luciferase reporter for circ_0004491 and GNAS. OSCC cells were co-transfected with above reporter vectors and miR-2278 or miR-NC mimic. To measure the luciferase activity, Dual-Lumi™ II Luciferase Assay Kit (Beyotime) was used.

RNA immunoprecipitation (RIP) assay

Magna RIP Kit (Millipore, Billerica, MA, USA) was implemented to perform RIP assay. Firstly, transfected OSCC cells were treated with RIP lysis buffer. Afterwards, magnetic beads pre-coated with antibodies against Ago2 (Anti-Ago2; 10686-1-AP, 1:50; Proteintech) or anti-IgG (16402-1-AP, 1:50; Proteintech) were added into cell lysates. The enrichment of circ_0004491 and miR-2278 was detected by qRT-PCR.

Xenograft model

BALB/c nude mice (5-week-old, female) were purchased from Vital River Laboratory (Beijing, China), and this study was permitted by the Animal Ethics Committee of Hanyang Hospital Affiliated to Medical College of Wuhan University of Science and Technology. CAL-27 cells transfected with vector or circ_0004491 were subcutaneously inoculated into the dorsal side of the mice (n = 5/group). On the 4th day after cells inoculation, tumor volume was firstly calculated, and the length (L) and width (W) of the forming tumors were measured every 4 days until 28th day. The volume (V) of the nodules was assessed according to the formula: $V\ (mm^3) = (L \times W^2)/2$. On the 28th day, tumors were taken out to be weighed and photographed. Tumor tissues of mice were collected to obtain total RNA and protein for qRT-PCR and western blotting. In addition, a part of tumor tissues were fixed to make paraffin-coated sections for immunohistochemistry (IHC). Antibody of ki67 in IHC was listed in Table 2.

Statistical analysis

Data were presented as the mean ± standard deviation and analyzed by paired or unpaired t test (two-tailed) or 1/2-way analysis of variance (ANOVA). Tukey's or Sidak's multiple comparisons test was performed after ANOVA. The correlations between circ_0004491, miR-2278 and GNAS were analyzed using Pearson correlation analysis. Statistical analysis was carried out using GraphPad Prism 8.0 software. A value $P < 0.05$ was considered to be significant.

Results

Circ_0004491 was downregulated in OSCC tissues and cell lines

Circ_0004491 was formed by the back-splicing of exon 2—-5 of ORC4 gene (Fig. 1A). Comparing to adjacent normal tissues, we found that the expression of circ_0004491 was obviously downregulated (Fig. 1B). The correlation between circ_0004491 expression and clinical characteristics in patients with OSCC was showed in Table 3. The expression of circ_0004491 was significantly correlated with tumor size and lymph-node metastasis. Thereafter, data showed that circ_0004491 expression was also significantly lower in OSCC cells (CAL-27, SCC-9, HSC-6 and OECM-1) than that in HOK cells (Fig. 1C). Further experiment showed that circ_0004491 could resist the digestion of RNase R, while linear ORC4 could be digested by RNase R (Fig. 1D and -E). After ActD treatment, we observed that the stability of circ_0004491 was higher than that of linear ORC4 (Fig. 1F and -G). These data confirmed that circ_0004491 had a circular structure, and might be implicated in the progression of OSCC.

Circ_0004491 suppressed OSCC cell proliferation and metastasis

To investigate the role of circ_0004491 in OSCC, circ_0004491 overexpression plasmid was transfected into OSCC cells and it evidently promoted circ_0004491 expression (Fig. 2A). To measure OSCC cells proliferation, colony formation assay and EdU staining were performed, and the results showed that circ_0004491 overexpression obviously reduced the colony numbers and the EdU positive cell rate (Fig. 2B and C). And the flow cytometry data showed that circ_0004491 overexpression promoted the apoptosis rate of CAL-27 and SCC-9 cells (Fig. 2D). Besides, circ_0004491 overexpression constrained the migrated the invaded cell number in CAL-27 and SCC-9 cells (Fig. 2E and F). To further confirm the above results, marker protein expression was detected, and the results indicated that overexpressed circ_0004491 promoted the protein expression of Bax and E-cadherin and decreased Bcl-2 protein expression in CAL-27 and SCC-9 cells (Fig. 2G and H). Besides that, circ_0004491 overexpression was accompanied with decreased N-cadherin and Vimentin in CAL-27 and SCC-9 cells (Figs. S1A—B). These outcomes suggested that circ_0004491 might suppress the progression of OSCC.

Circ_0004491 served as miR-2278 sponge

Using the starBase online software, we found that miR-2278 possessed complementary binding sites with circ_0004491. And according to the binding sites between circ_0004491 and miR-2278, the circ_0004491 WT/MUT vectors were constructed (Fig. 3A). After confirming that miR-2278 mimic indeed promoted miR-2278 expression (Fig. 3B), miR-2278 mimic and the circ_0004491 WT/MUT vectors were co-transfected into CAL-27 and SCC-9 cells. Dual-luciferase reporter assay results revealed that overexpressed miR-2278 only reduced the luciferase activity of circ_0004491 WT vector without affecting that of the circ_0004491 MUT vector (Fig. 3C and D). Moreover, RIP assay results showed that circ_0004491 and miR-2278 could be markedly enriched in Anti-Ago2-preincubated beads (Fig. 3E and F). The expression of miR-2278 was significantly upregulated in OSCC tissues and cells (CAL-27 and SCC-9) when compared with adjacent normal tissues and HOK cells (Fig. 3G and H). And there was a negative correlation between the expression of circ_0004491 and miR-2278 in OSCC tumor tissues

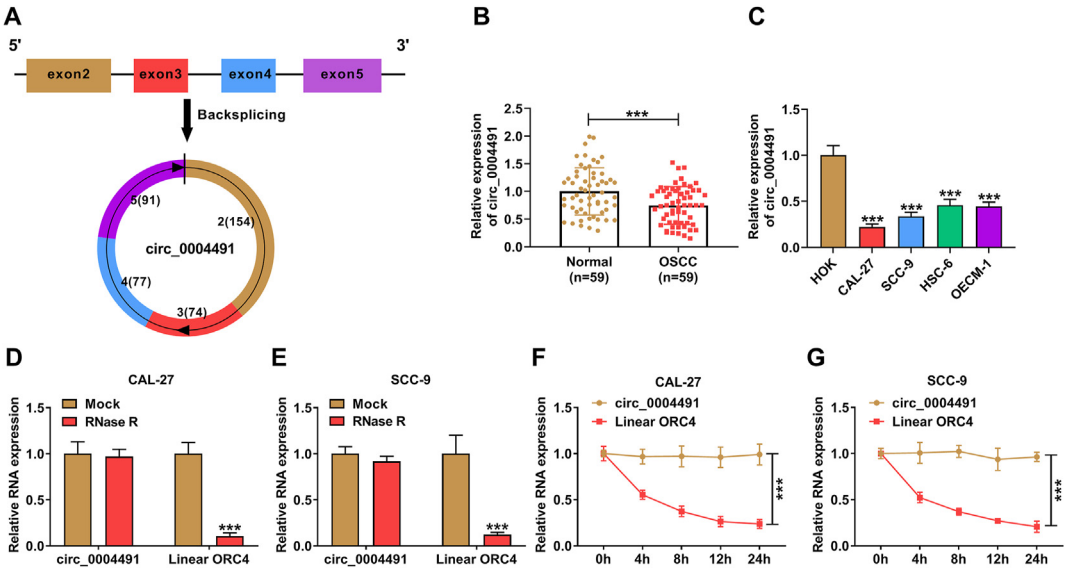

Fig. 1 Circ_0004491 expression was downregulated in the tissues and cell lines of OSCC. (A) The basic information of circ_0004491 was shown. (B) The expression of circ_0004491 was measured by qRT-PCR analysis in clinical OSCC tumor and adjacent normal tissues (N = 59). (C) Circ_0004491 expression was detected by qRT-PCR analysis in OSCC cell lines (CAL-27, SCC-9, HSC-6 and OECM-1) and HOK cell line. (D–G) RNase R assay (D–E) and Act D assay (F–G) were performed to identify the circular characteristic of circ_0004491. ***$P < 0.001$.

Table 3 Correlation between clinicopathologic parameters of OSCC patients and circ_0004491 expression.

Parameter	Case	Circ_0004491 expression		*P* value
		Low ($n = 29$)	High ($n = 30$)	
Sex				0.522
Male	33	15	18	
Female	26	14	12	
Age (years)				0.506
≤60	27	12	15	
>60	32	17	15	
Tumor size				0.013*
≤4 cm	31	20	11	
>4 cm	28	9	19	
Differentiation				0.366
Good/moderate	23	13	10	
Poor	36	16	20	
Lymph-node metastasis				0.006*
Yes	26	18	8	
No	33	11	22	

*$P < 0.05$.

(Fig. 3I). These data revealed that circ_0004491 acted as a molecular sponge for miR-2278.

Circ_0004491 regulated OSCC progression by sponging miR-2278

The rescue experiments were performed to explore whether circ_0004491 regulated OSCC progression by sponging miR-2278. Circ_0004491 and miR-2278 were co-transfected into CAL-27 and SCC-9 cells. The results showed that circ_0004491 overexpression obviously repressed miR-2278 expression, miR-2278 mimic reverted this inhibitory effects (Fig. 4A). And miR-2278 mimic could promote the colony number and the EdU positive cell rate and restrained cell apoptosis rate in circ_0004491-depressed cells (Fig. 4B–D). Besides, the negative regulation of circ_0004491 overexpression on the migration and invasion of CAL-27 and SCC-9 cells was also overturned by miR-2278 mimic (Fig. 4E–H). Furthermore, the detection of protein levels displayed that the promotion effect of overexpressed circ_0004491 on the protein expression of Bax and E-cadherin and the repression effect on Bcl-2 protein expression were reversed by miR-2278 mimic (Fig. 4I and J). All results indicated that circ_0004491 suppressed OSCC progression by sponging miR-2278.

MiR-2278 directly targeted GNAS

The target of miR-2278 was predicted by the starBase online software, and the binding sites of GNAS 3'UTR and miR-2278 were showed. Then, the GNAS 3'UTR WT/MUT vectors were synthesized (Fig. 5A). After co-transfected with the miR-2278 mimic and GNAS 3'UTR WT/MUT vectors into CAL-27 and SCC-9 cells, we discovered that miR-2278 mimic reduced the luciferase activity of GNAS 3'UTR WT vector, while had not effect on that of the GNAS 3'UTR MUT vector (Fig. 5B and C). These outcomes confirmed the interaction between miR-2278 and GNAS. By detecting GNAS mRNA and protein level expression, we found that GNAS expression was downregulated in OSCC tumor tissues and cells (Fig. 5D–F). Additionally, circ_0004491 overexpression evidently promoted the protein expression of GNAS, and this effect was reverted by miR-2278 mimic (Fig. 5G–I).

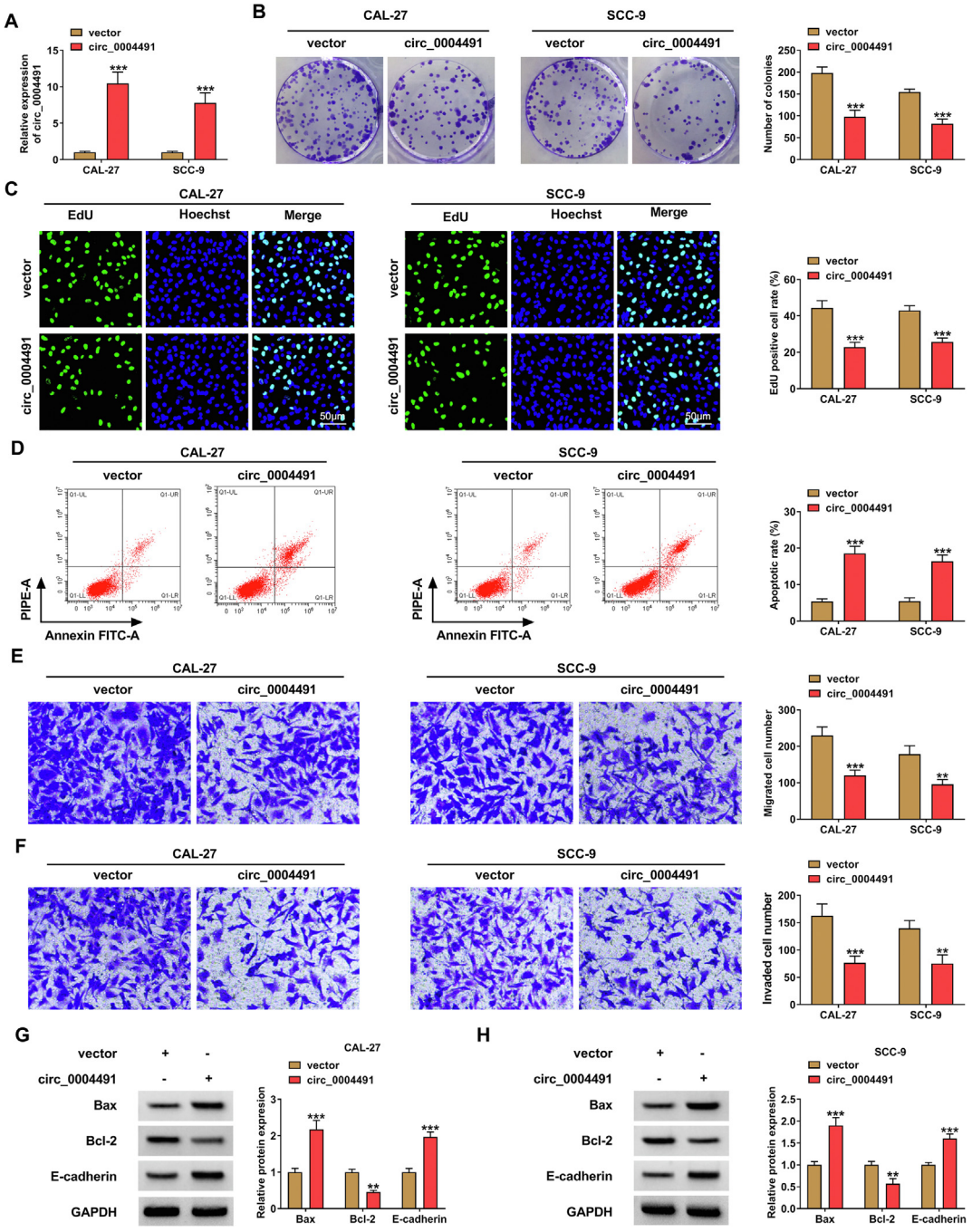

Fig. 2 Circ_0004491 repressed the malignant behaviors of OSCC cells. CAL-27 and SCC-9 cells were transfected with circ_0004491 or vector. (A) The expression of circ_0004491 was examined by qRT-PCR analysis to confirm transfection efficiency. (B—C) Colony formation assay (B) and EdU staining (C) were performed to investigate the proliferation ability of OSCC cells. (D) The cell apoptosis rate was determined by flow cytometry. (E—F) Transwell assay was used to examine cell migration and invasion. (G—H) The protein levels of Bax, Bcl-2 and E-cadherin were detected by western blotting. $^{**}P < 0.01$ and $^{***}P < 0.001$.

Correlation analysis revealed that GNAS mRNA expression was negatively correlated with miR-2278 expression, and positively correlated with circ_0004491 expression in OSCC tumor tissues (Fig. 5J and K). Taken together, we confirmed that circ_0004491 could sponge miR-2278 to positively regulate GNAS.

MiR-2278 inhibitor-mediated effects were overturned by GNAS knockdown in OSCC cells

The transfection efficiencies of in-miR-2278 and sh-GNAS in OSCC cells were verified by qRT-PCR and western blotting, respectively (Fig. 6A and B). Then, we co-transfected in-

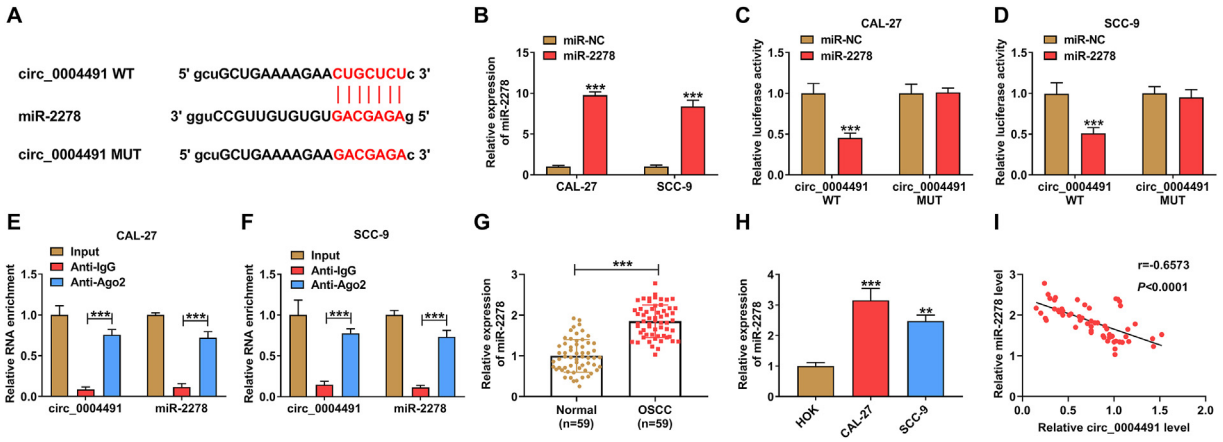

Fig. 3 Circ_0004491 interacted with miR-2278 in OSCC cells. (A) The predicted miR-2278-binding sites in circ_0004491 WT and MUT were showed. (B) The expression of miR-2278 was examined by qRT-PCR analysis to confirm transfection efficiency. (C–D) The relative luciferase activity of circ_0004491 WT and MUT reporter vectors was measured by dual-luciferase reporter assay. (E–F) The relative RNA enrichment of circ_0004491 and miR-2278 was detected by RIP assay. (G) MiR-2278 expression was tested by qRT-PCR analysis in clinical OSCC tumor and adjacent normal tissues (N = 59). (H) The expression of miR-2278 was determined by qRT-PCR analysis in HOK, CAL-27 and SCC-9 cells. (I) Pearson correlation analysis was performed between relative circ_0004491 and miR-2278 levels in OSCC tumor tissues. $^{**}P < 0.01$ and $^{***}P < 0.001$.

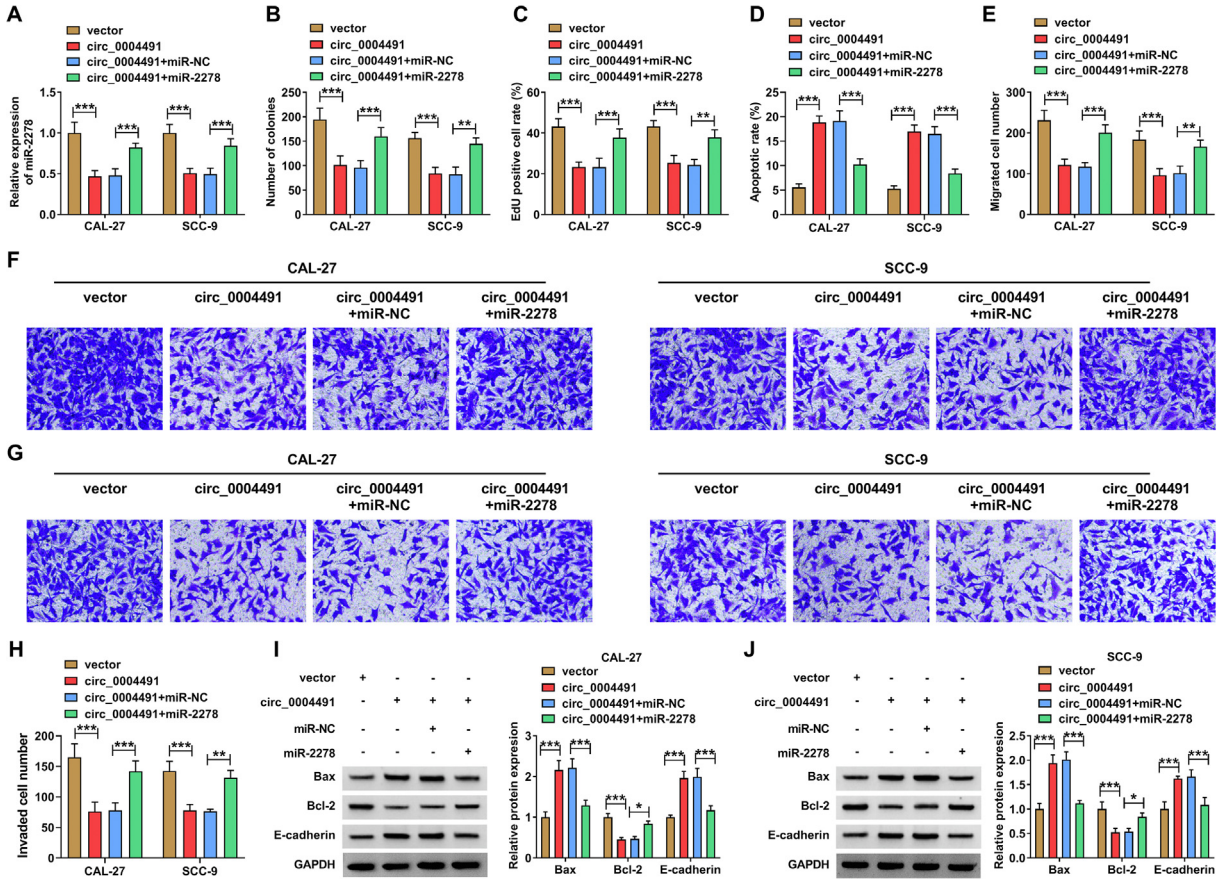

Fig. 4 MiR-2278 mimic overturned circ_0004491 overexpression-mediated effect in OSCC cells. CAL-27 and SCC-9 cells were transfected with vector or circ_0004491 and miR-NC or miR-2278. (A) The expression of miR-2278 was measured by qRT-PCR analysis. (B–C) Colony formation assay (B) and EdU staining (C) were performed to investigate the proliferation ability of OSCC cells. (D) The cell apoptosis rate was determined by flow cytometry. (E–H) Transwell assay was used to examine cell migration and invasion. (I–J) The protein levels of Bax, Bcl-2 and E-cadherin were detected by western blotting. $^{*}P < 0.05$, $^{**}P < 0.01$ and $^{***}P < 0.001$.

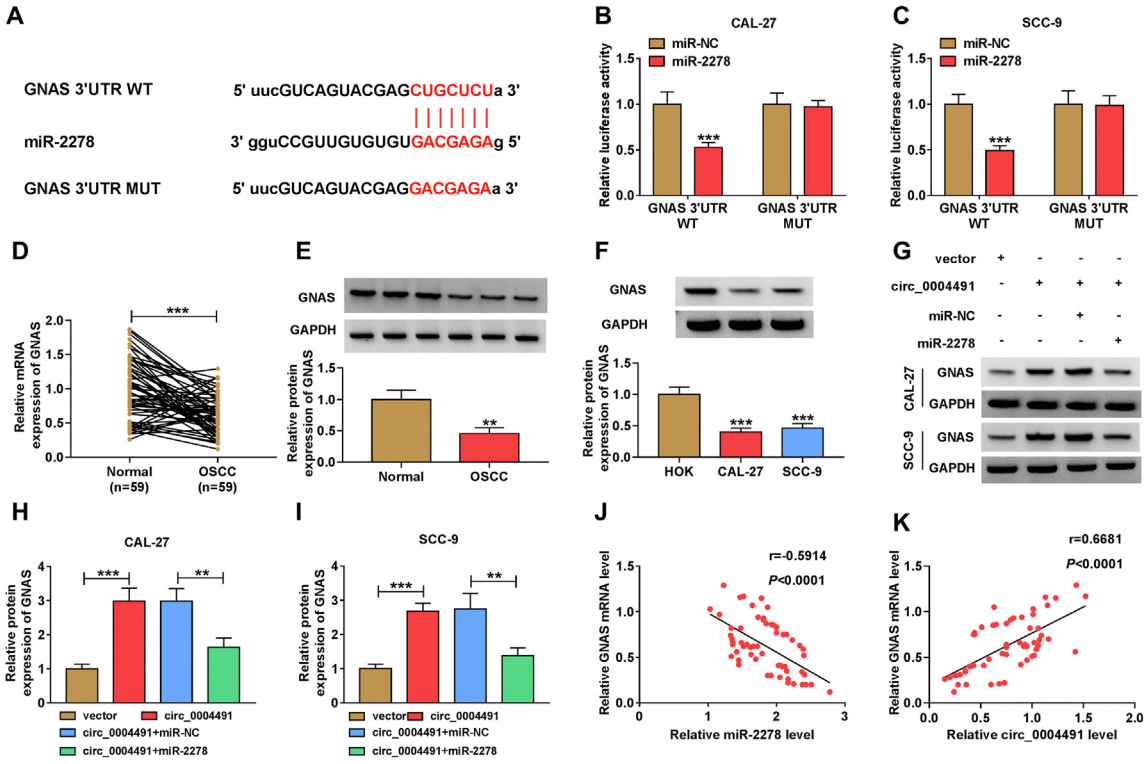

Fig. 5 MiR-2278 interacted with GNAS in OSCC cells. (A) The predicted miR-2278-binding sites in GNAS 3'UTR WT and MUT were showed. (B–C) The relative luciferase activity of GNAS 3'UTR WT and MUT reporter vectors was measured by dual-luciferase reporter assay. (D–E) The expression of GNAS was tested by qRT-PCR analysis and western blotting in clinical OSCC tumor and adjacent normal tissues (N = 59). (F) The expression of GNAS was determined by western blotting in HOK, CAL-27 and SCC-9 cells. (G–I) GNAS protein level was determined by western blotting in CAL-27 and SCC-9 cells transfected with vector or circ_0004491 and miR-NC or miR-2278. (J–K) Pearson correlation analysis was performed between relative GNAS level and miR-2278 or circ_0004491 levels in OSCC tumor tissues. $^{**}P < 0.01$ and $^{***}P < 0.001$.

miR-2278 and sh-GNAS into CAL-27 and SCC-9 cells to conduct rescue experiments, and results revealed that in-miR-2278-induced upregulation in GNAS protein level was restored by GNAS knockdown (Fig. 6C). For functional experiments, data showed that miR-2278 inhibitor suppressed the colony number and the EdU positive cell rate and facilitated cell apoptosis rate, and GNAS silencing reverted the above effect (Fig. 6D–F). Besides, the inhibitory effect of miR-2278 inhibitor on the migration and invasion of CAL-27 and SCC-9 cells was also restored by GNAS knockdown (Fig. 6G–I). Furthermore, GNAS silencing also overturned the upregulation of Bax and E-cadherin protein expression and the repression of Bcl-2 protein expression mediated by miR-2278 inhibitor (Fig. 6J and K). Therefore, we verified that miR-2278 regulated cell proliferation and metastasis of OSCC cells by targeting GNAS.

Overexpressed circ_0004491 inhibited OSCC tumor growth *in vivo*

The xenograft tumor experiment was employed to further confirm the role of circ_0004491 in OSCC tumorigenesis *in vivo*. As revealed in Fig. 7A–C, circ_0004491 overexpression restrained the tumor volume and weight when comparing with the vector group. Besides, overexpressed circ_0004491 contributed to the expression of circ_0004491 and GNAS, while hindered miR-2278 expression (Fig. 7D–F). IHC staining results showed that the positive cells of ki-67 in the tumor tissues of circ_0004491 overexpression group was lower than that in the tumor tissues of vertor group (Fig. 7G). These findings displayed that circ_0004491 acted as a tumor suppressor in OSCC.

Discussion

The incidence of OSCC is increasing year by year.[18] Despite treatment plan has been improved, the prognosis of patients was still unsatisfactory.[1] In this study, the data confirmed that the expression of circ_0004491 was lower in OSCC tumor tissues and cell lines than that in controls. Overexpressed circ_0004491 significantly reduced the cell growth, motility, whereas contributed to cell apoptosis of OSCC. In addition, circ_0004491, as a competing endogenous RNA (ceRNA), promoted GNAS expression through sponging miR-2278, thereby inhibiting tumor growth and metastasis.

The application of targeted therapy provided new ideas for cancer therapy.[19,20] Finding effective biomarkers and

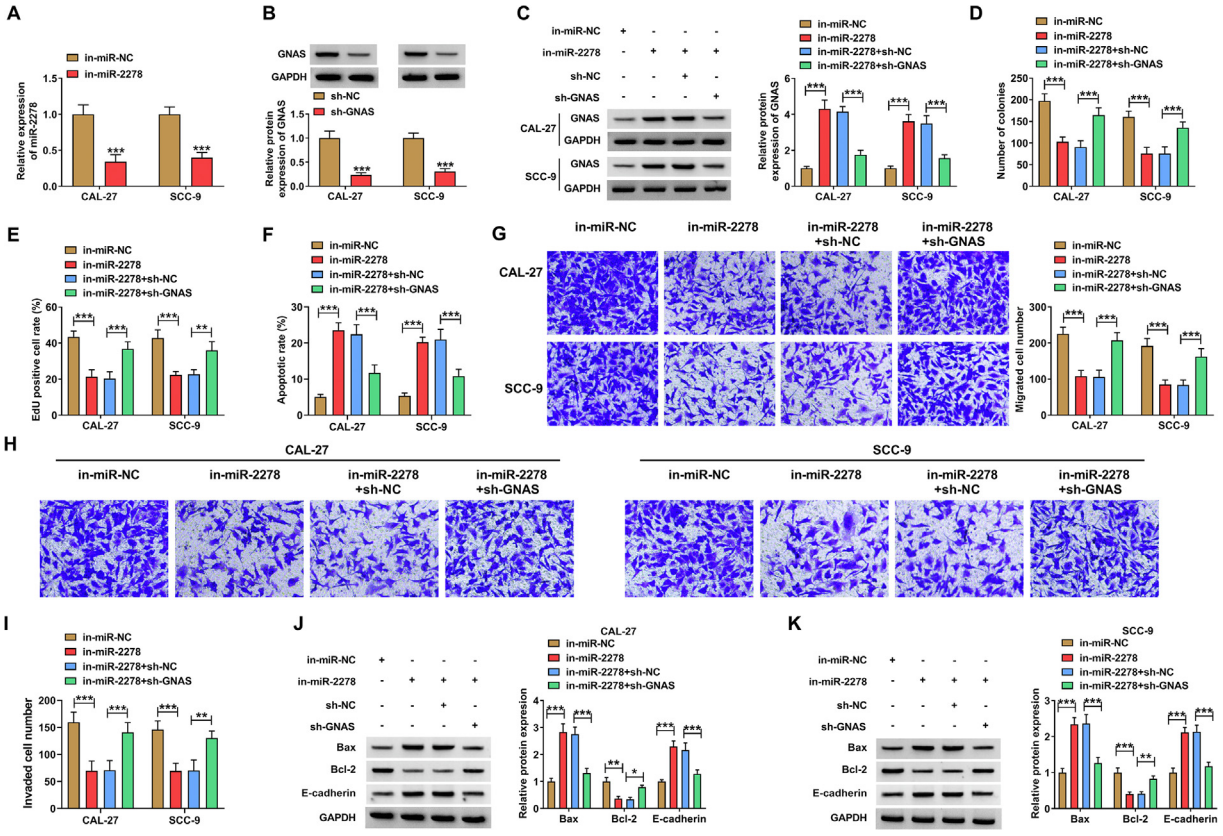

Fig. 6 MiR-2278 inhibitor-mediated effect was restored by GNAS knockdown in OSCC cells. (A–B) The expression of miR-2278 and GNAS were examined by qRT-PCR analysis and western blotting respectively to confirm transfection efficiency. Then, CAL-27 and SCC-9 cells were transfected with in-miR-NC, in-miR-2278, in-miR-2278+sh-NC or in-miR-2278+sh-GNAS. (C) The expression of GNAS was detected by western blotting. (D–E) Colony formation assay (D) and EdU staining (E) were performed to investigate the proliferation ability of OSCC cells. (F) The cell apoptosis rate was determined by flow cytometry. (G–I) Transwell assay was used to examine cell migration and invasion. (J–K) The protein levels of Bax, Bcl-2 and E-cadherin were detected by western blotting. $^{*}P < 0.05$, $^{**}P < 0.01$ and $^{***}P < 0.001$.

therapeutic targets was crucial for the diagnosis of early OSCC and the treatment of advanced OSCC. Through RNA sequencing, the differential expression of circRNA has been proved to be involved in the process of OSCC.[21,22] With the deepening of research, the pro-cancer and anti-cancer role of some circRNA has been revealed in the progress of OSCC.[23–25] For instance, Circ-PVT1 facilitated OSCC development through mediating miR-106a-5p/HK2 axis.[23] Hsa_circ_0007059 was reported to be obviously down-regulated in OSCC, and it improved OSCC by modulating AKT/mTOR signal pathway.[24] Circ-PKD2 repressed APC2 expression and OSCC carcinogenesis via absorbing miR-204-3p.[25] In this study, we focused on the role of circ_0004491 in OSCC progress. Consistent with previous studies, circ_0004491 expression in OSCC tissues and cell lines was apparently reduced comparing to the controls and had an inhibitory effect on cell metastasis. The difference was that we also confirmed that circ_0004491 overexpression evidently constrained cell proliferation and facilitated cell apoptosis. Moreover, by establishing a mouse xenograft model, the inhibitory effect of circ_0004491 on the growth of OSCC cells was also verified *in vivo*.

As reported, circRNA acted as the ceRNA of miRNA to regulate cell biological functions.[26] For instance, Li et al. proved that circ_0004491 could interact with miR-155-5p using bioinformatics analysis combined with qRT-PCR experiment.[13] Through bioinformatics analysis, Guo et al. found that circ_0001971 had binding sites with miR-194 and miR-204, and it was verified by dual-luciferase reporter gene and RIP assays that circ_0001971 could sponge miR-194 and miR-204.[27] Following the previous methods, we used bioinformatics prediction, dual-luciferase reporter gene and RIP experiments to prove that circ_0004491 acted as a ceRNA of miR-2278. In addition, miR-2278 has been found to be upregulated and played a tumor-promoting role in cancers.[14,15] For example, Wang et al. proved that overexpression of long non-coding RNA ASAP1IT1 could contribute to LATS2 protein expression whereas suppress ovarian cancer process by sponging miR-2278.[14] In OSCC, the expression and function of miR-2278 have not been studied. Our study confirmed that miR-2278 was highly

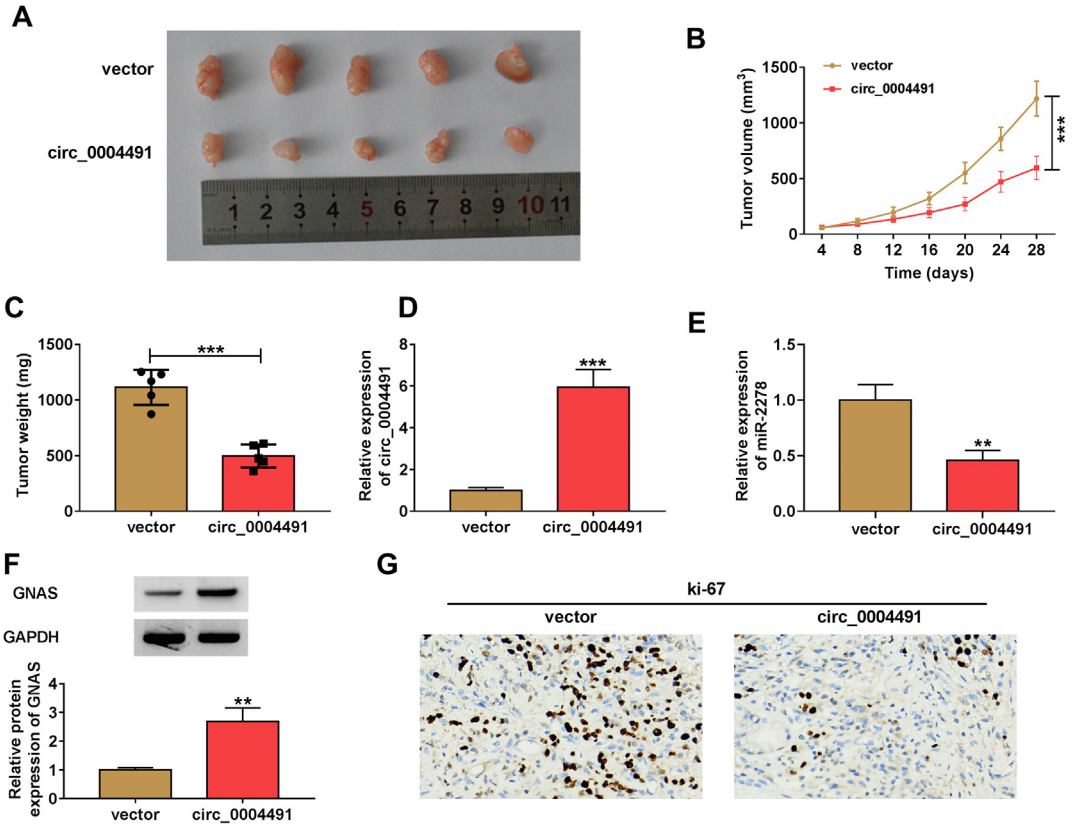

Fig. 7 Role of circ_0004491 overexpression in tumorigenicity of OSCC cells *in vivo*. CAL-27 cells stably transfected with vector or circ_0004491 were injected into nude mice (n = 5/group) to induce xenograft tumors. (A) The most representative tumors were presented. (B) Tumor volume was monitored at an interval of 4 days. (C) Tumor weight was evaluated on the 28th day. (D—F) Circ_0004491 and miR-2278 expression were measured by qRT-PCR analysis (D—E), and the relative protein expression of GNAS was detected by western blotting (F). (G) The ki-67 positive cells were stained by IHC assay. $^{**}P < 0.01$ and $^{***}P < 0.001$.

expressed in OSCC and played an important role in promoting proliferation and metastasis in OSCC for the first time. The results of the rescue experiments showed that miR-2278 ameliorated the repressive effect of circ_0004491 on the process of OSCC, demonstrating that miR-2278 had a positive regulatory effect on the malignant behaviors of OSCC cells.

As a negative gene regulator, miRNA regulated cell metabolism, proliferation, differentiation, apoptosis and other biological functions by suppressing target gene expression.[28] StarBase database was used for bioinformatics prediction and the prediction result indicated that miR-2278 and GNAS had targeted binding sites in the sequence. Subsequently, dual-luciferase reporter gene experiment confirmed the binding relationship of miR-2278 and GNAS in OSCC cells. It has been reported that the expression of GNAS in osteoporotic (OP) mice was significantly reduced comparing with normal mice, and miR-196a mimic could inhibit the expression of GNAS and promote the osteogenic differentiation by activating the hedgehog signaling pathway.[29] GNAS has been showed to be widely altered across cancer types.[30] Moreover, abnormal expressed GNAS was involved in regulating the tumorgenesis of many of cancers, such as hepatocellular carcinoma, breast cancer, and OSCC.[17,31,32] The data of this study showed that GNAS knockdown could restore miR-2278 inhibitor-mediated inhibitory effect on the malignant behaviors of OSCC cells, indicating that miR-2278 inhibitor partially inhibited OSCC progression by up-regulating GNAS expression.

In conclusion, circ_0004491/miR-2278/GNAS axis was identified for the first time in our study. Circ_0004491 repressed the malignant phenotypes of OSCC cells by binding with miR-2278 to induce GNAS expression, which provided new ideas for OSCC molecular targeted therapy.

Declaration of competing interest

The authors declare that they have no known competing financial interests or personal relationships that could have appeared to influence the work reported in this paper.

Acknowledgements

None.

Appendix A. Supplementary data

Supplementary data to this article can be found online at https://doi.org/10.1016/j.jds.2022.05.018.

References

1. Lorini L, Bescos Atin C, Thavaraj S, et al. Overview of oral potentially malignant disorders: from risk factors to specific therapies. *Cancers* 2021;13:3696.
2. Thomson PJ. Perspectives on oral squamous cell carcinoma prevention-proliferation, position, progression and prediction. *J Oral Pathol Med* 2018;47:803—7.
3. Shen ZS, Li JS, Chen WL, Fan S. The latest advancements in selective neck dissection for early stage oral squamous cell carcinoma. *Curr Treat Options Oncol* 2017;18:31.
4. Gamez ME, Kraus R, Hinni ML, et al. Treatment outcomes of squamous cell carcinoma of the oral cavity in young adults. *Oral Oncol* 2018;87:43—8.
5. Wang R, Wang Y. Fourier transform infrared spectroscopy in oral cancer diagnosis. *Int J Mol Sci* 2021;22:1206.
6. Olmos M, Glajzer J, Buntemeyer TO, et al. Neoadjuvant immunotherapy of oral squamous cell carcinoma: case report and assessment of histological response. *Front Oncol* 2021;11:720951.
7. Tang X, Ren H, Guo M, Qian J, Yang Y, Gu C. Review on circular RNAs and new insights into their roles in cancer. *Comput Struct Biotechnol J* 2021;19:910—28.
8. Qin T, Li J, Zhang KQ. Structure, regulation, and function of linear and circular long non-coding RNAs. *Front Genet* 2020;11:150.
9. Garlapati P, Ling J, Chiao PJ, Fu J. Circular RNAs regulate cancer-related signaling pathways and serve as potential diagnostic biomarkers for human cancers. *Cancer Cell Int* 2021;21:317.
10. Chen X, Yu J, Tian H, et al. Circle RNA hsa_circRNA_100290 serves as a ceRNA for miR-378a to regulate oral squamous cell carcinoma cells growth via Glucose transporter-1 (GLUT1) and glycolysis. *J Cell Physiol* 2019;234:19130—40.
11. Huang Y, Zhang C, Xiong J, Ren H. Emerging important roles of circRNAs in human cancer and other diseases. *Genes Dis* 2021;8:412—23.
12. Li J, Sun D, Pu W, Wang J, Peng Y. Circular RNAs in cancer: biogenesis, function, and clinical significance. *Trends Cancer* 2020;6:319—36.
13. Li X, Zhang H, Wang Y, Sun S, Shen Y, Yang H. Silencing circular RNA hsa_circ_0004491 promotes metastasis of oral squamous cell carcinoma. *Life Sci* 2019;239:116883.
14. Wang K, Hu YB, Zhao Y, Ye C. Long noncoding RNA ASAP1IT1 suppresses ovarian cancer progression by regulating Hippo/YAP signaling. *Int J Mol Med* 2021;47:44.
15. Borrego-Diaz E, Powers BC, Azizov V, et al. A potential regulatory loop between Lin28B:miR212 in androgen-independent prostate cancer. *Int J Oncol* 2014;45:2421—9.
16. Cong Q, Xu R, Yang Y. Galphas signaling in skeletal development, homeostasis and diseases. *Curr Top Dev Biol* 2019;133:281—307.
17. Zhu X, Shao P, Tang Y, Shu M, Hu WW, Zhang Y. hsa_circRNA_100533 regulates GNAS by sponging hsa_miR_933 to prevent oral squamous cell carcinoma. *J Cell Biochem* 2019;120:19159—71.
18. Wong YL, Ramanathan A, Yuen KM, et al. Comparative sera proteomics analysis of differentially expressed proteins in oral squamous cell carcinoma. *PeerJ* 2021;9:e11548.
19. Toden S, Zumwalt TJ, Goel A. Non-coding RNAs and potential therapeutic targeting in cancer. *Biochim Biophys Acta Rev Cancer* 2021;1875:188491.
20. Li J, Sun D, Pu W, Wang J, Peng Y. Circular RNAs in cancer: biogenesis, function, and clinical significance. *Trends Cancer* 2020;6:319—36.
21. Shao Y, Song Y, Xu S, Li S, Zhou H. Expression profile of circular RNAs in oral squamous cell carcinoma. *Front Oncol* 2020;10:533616.
22. Zhang B, Wang Z, Shen Y, Yang H. Silencing circular RNA hsa_circ_009755 promotes growth and metastasis of oral squamous cell carcinoma. *Genomics* 2020;112:5275—81.
23. Zhu X, Du J, Gu Z. Circ-PVT1/miR-106a-5p/HK2 axis regulates cell growth, metastasis and glycolytic metabolism of oral squamous cell carcinoma. *Mol Cell Biochem* 2020;474:147—58.
24. Su W, Wang Y, Wang F, et al. Circular RNA hsa_circ_0007059 indicates prognosis and influences malignant behavior via AKT/mTOR in oral squamous cell carcinoma. *J Cell Physiol* 2019;234:15156—66.
25. Gao L, Zhao C, Li S, et al. circ-PKD2 inhibits carcinogenesis via the miR-204-3p/APC2 axis in oral squamous cell carcinoma. *Mol Carcinog* 2019;58:1783—94.
26. Qi X, Zhang DH, Wu N, Xiao JH, Wang X, Ma W. ceRNA in cancer: possible functions and clinical implications. *J Med Genet* 2015;52:710—8.
27. Tan X, Zhou C, Liang Y, Lai YF, Liang Y. Circ_0001971 regulates oral squamous cell carcinoma progression and chemosensitivity by targeting miR-194/miR-204 in vitro and in vivo. *Eur Rev Med Pharmacol Sci* 2020;24:2470—81.
28. Salim U, Kumar A, Kulshreshtha R, Vivekanandan P. Biogenesis, characterization, and functions of mirtrons. *Wiley Interdiscip Rev RNA* 2022;13:e1680.
29. Zhong LN, Zhang YZ, Li H, Fu HL, Lv CX, Jia XJ. Overexpressed miR-196a accelerates osteogenic differentiation in osteoporotic mice via GNAS-dependent Hedgehog signaling pathway. *J Cell Biochem* 2019;120:19422—31.
30. Parish AJ, Nguyen V, Goodman AM, Murugesan K, Frampton GM, Kurzrock R. GNAS, GNAQ, and GNA11 alterations in patients with diverse cancers. *Cancer* 2018;124:4080—9.
31. Ding H, Zhang X, Su Y, Jia C, Dai C. GNAS promotes inflammation-related hepatocellular carcinoma progression by promoting STAT3 activation. *Cell Mol Biol Lett* 2020;25:8.
32. Jin X, Zhu L, Cui Z, Tang J, Xie M, Ren G. Elevated expression of GNAS promotes breast cancer cell proliferation and migration via the PI3K/AKT/Snail1/E-cadherin axis. *Clin Transl Oncol* 2019;21:1207—19.